Journal of Thermal Analysis and Calorimetry, Vol. 96 (2009) 2, 469–474

THERMAL BEHAVIOUR AND PROPERTIES OF Na_2O–TiO_2–P_2O_5 GLASSES

P. Mošner[*]*, K. Vosejpková and L. Koudelka*

Department of General and Inorganic Chemistry, Faculty of Chemical Technology, University of Pardubice, 532 10 Pardubice, Czech Republic

Differential scanning calorimetry (DSC) and thermomechanical analysis (TMA) were used to study the thermal behaviour of $(50–x)Na_2O–xTiO_2–50P_2O_5$ and $45Na_2O–yTiO_2–(55–y)P_2O_5$ glasses. The addition of TiO_2 to the starting glasses (x=0 and y=5 mol% TiO_2) resulted in a nonlinear increase of glass transition temperature and dilatation softening temperature, whereas the thermal expansion coefficient decreased. All prepared glasses crystallize under heating within the temperature range of 300–610°C. The contribution of the surface crystallization mechanism over the internal one increases with increasing TiO_2 content. With increasing TiO_2 content the temperature of maximum nucleation rate is also gradually shifted from a value close to the glass transition temperature towards the crystallization temperature. X-ray diffraction measurements showed that the major compounds formed by glass crystallization were $NaPO_3$, TiP_2O_7 and $NaTi_2(PO_4)_3$. The chemical durability of the glasses without titanium oxide is very poor, but with the replacement of Na_2O or P_2O_5 by TiO_2, it increases sharply.

Keywords: *DSC, glasses, thermal expansion, X-ray diffraction*

Introduction

Titanophosphate glasses and glass-ceramics have been extensively studied in recent years because of their potential applications as solid electrolytes, waveguides, bio-implants, optical switches and fibres or power limiters [1–4].

The addition of TiO_2 to phosphate glasses improves their chemical durability, thermal stability and other physical properties [1, 2, 5, 6]. These changes are due to the incorporation of TiO_x structural units into the phosphate structural network, which is accompanied by the depolymerisation of this network and the formation of Ti–O–P bonds [7–9]. At high TiO_2 content, Ti–O–Ti bonds and the NASICON (Na Super Ionic CONductor) type structure can be formed in the crystallized glasses [7].

The aim of the present study was to prepare glassy samples of the $Na_2O–TiO_2–P_2O_5$ system and to investigate compositional changes in their physico-chemical properties (especially thermal behaviour).

Experimental

Sodium titanophosphate glasses with the composition $(50–x)Na_2O–xTiO_2–50P_2O_5$ (compositional series A) and $45Na_2O–yTiO_2–(55–y)P_2O_5$ (B) were prepared in batches of 50 g using analytical-grade Na_2CO_3, TiO_2 (anatase) and H_3PO_4. The starting mixture was heated slowly to 1260–1320°C in a platinum crucible with a lid. After 15 min at the maximum temperature, the resulting melt was cooled slowly in a graphite mould or quenched between two copper blocks. The glasses obtained were annealed for 15 min at the temperature 5°C below their glass transition temperature, T_g.

The glass density, ρ, was determined in bulk samples by the Archimedes method using CCl_4 as the immersion liquid. The molar volume, V_M, was calculated as $V_M = \overline{M}/\rho$, where $\overline{M}$ is the average molar mass of the glass composition $xNa_2O–yTiO_2–zP_2O_5$ calculated for $x+y+z=1$. The chemical durability of the glasses was evaluated from the measurements of the dissolution rate, DR, at 25°C. The measurement of DR was conducted on glass cubes with dimensions of 5×5×5 mm. These cubes were shaken in 100 cm^3 of water for 1 h. Before and after the dissolution test the samples were dried at 105°C. The dissolution rate, DR, was calculated from the expression $DR=\Delta\omega/St$, where $\Delta\omega$ is the mass loss [g], S is the sample area [cm^2] before the dissolution test and t is the dissolution time [min].

The thermal behaviour of glasses was studied with the DTA 404 PC (Netzsch) operating in the DSC mode at the heating rate of 10°C min^{-1}. The measurement was carried out on powder samples with a mean diameter 8–10 μm placed in corundum crucibles under an atmosphere of N_2. The thermal expansion coefficient, α, the glass transition temperature, T_g, and dilatation softening temperature, T_d, were measured on the cubes with dimensions of 5×5×5 mm using TMA equipment (RMI

---

[*] Author for correspondence: petr.mosner@upce.cz

1388–6150/$20.00

Akadémiai Kiadó, Budapest, Hungary
Springer, Dordrecht, The Netherlands

Pardubice) at the heating rate of 10°C min^{-1}. Samples were analysed in air between two quartz plates subjected to compressive force of 10 mN. From the obtained dilatation curves the coefficient of thermal expansion, α, was determined as a mean value in the temperature range of 150–250°C, the glass transition temperature, T_g, was determined from the change in the slope of the elongation *vs*. temperature plot and the dilatation softening temperature, T_d, was obtained from the maximum of the expansion trace corresponding to the onset of viscous deformation.

Crystalline phases were identified by X-ray powder diffraction analysis with a Bruker D8 Advance diffractometer using powder samples. Crystalline samples were prepared using isothermal heating in the temperature range of 300–580°C for glasses with composition $(50–x)Na_2O–xTiO_2–50P_2O_5$ (A) and 580–610°C for glasses with composition $45Na_2O–yTiO_2–(55–y)P_2O_5$ (B) in a graphite mould for 2 h under an inert atmosphere (N_2).

For the evaluation of the nucleation rate, 50 mg of the glass with the average particle size of 300 μm was first heated in DTA equipment from room temperature to a nucleation temperature, T_N, between the glass transition temperature, T_g, and the crystallization temperature, T_c (onset of the first crystallization peak) and then nucleated at T_N for 30 min. After subsequent cooling to 100°C, the sample was heated again to the temperature above the crystallization peaks at a rate of 10°C min^{-1}. This process was applied gradually for several nucleation temperatures. At the temperature corresponding to maximum nucleation, determined in the previous step from the plot of crystallization peak height, $(\delta T)_p$ *vs.* T_N, the glass was then heat treated for 15–75 min.

Results and discussion

By the procedure described above, eight homogeneous glasses in the compositional series A: $(50–x)Na_2O–xTiO_2–50P_2O_5$ (x=0, 2.5, 5, 7.5 and 10 mol% TiO_2) and B: $45Na_2O–yTiO_2–(55–y)P_2O_5$ (y=5, 10, 15, 20 mol% TiO_2) were prepared. All glasses except the glass with composition $40Na_2O–10TiO_2–50P_2O_5$ which was prepared by quenching between two copper blocks, were prepared by slow cooling of the melt in air. The presence of a glassy state was checked by X-ray diffraction. The obtained compositional range corresponds to glass forming regions in $Na_2O–TiO_2–P_2O_5$ systems described by Kishioka *et al.* [10]. The colour of the glasses slowly changed from clear to yellowish and brown with increasing TiO_2 content.

Determined values of the glass density, ρ, and molar volume, V_M, are given in Table 1. As can be seen the glass density of the studied glasses increases slightly with increasing TiO_2 content. The molar volume is practically constant in compositional series $(50–x)Na_2O–xTiO_2–50P_2O_5$ (A) while in the series $45Na_2O–yTiO_2–(55–y)P_2O_5$ (B) decreases with increasing TiO_2 content.

The values of the dissolution rate, *DR*, obtained (Table 1) show that the chemical durability steeply increases with the replacement of Na_2O and P_2O_5 by TiO_2, in both compositional series of glasses. The reason for the increase of chemical stability with the replacement of Na_2O by TiO_2 in compositional series A is the change of polarity of M–O bonds when the Ti^{4+} ions with small ionic radius and high electrical charge contribute to the formation of stronger P–O–M bonds than Na^+ ions. The Ti^{4+} ions are in competition with the Na^+ ions and occupy sites close to the PO_4 end groups. In this way they block the migration paths of

Table 1 Density, ρ, molar volume, V_M, dissolution rate, DR, glass transition temperature, T_g, dilatation softening temperature, T_d, crystallization temperature, T_c, melting temperature, T_m, and thermal expansion coefficient, α, of $Na_2O–TiO_2–P_2O_5$ glasses

Na_2O	TiO_2	P_2O_5	$\rho\pm0.02$	V_M	$DR\cdot10^7$	$T_g\pm2^a$	$T_c\pm2^a$	$T_m\pm2^a$	$T_g\pm2^b$	$T_d\pm2^b$	$\alpha\pm0.5^b$	T_g/T_m
	mol%		g cm^{-3}	$\mathrm{cm}^3\ \mathrm{mol}^{-1}$	g $\mathrm{cm}^{-2}\ \mathrm{min}^{-1}$			°C			ppm °C^{-1}	
50	0	50	2.49	40.9	1323	288	316	610	–	–	–	0.47
47.5	2.5	50	2.52	40.7	1335	297	362	602	294	314	25.5	0.49
45	5	50	2.53	40.7	21	310	432	600	307	329	22.0	0.52
42.5	7.5	50	2.54	40.7	10	316	428	599	312	332	21.7	0.53
40	10	50	2.57	40.4	14	327	464	592	326	356	21.4	0.55
45	5	50	2.53	40.7	21	310	432	600	307	329	22.0	0.52
45	10	45	2.57	38.9	5	334	460	602	330	374	21.9	0.56
45	15	40	2.63	36.7	3	392	457	606	388	430	16.7	0.65
45	20	35	2.71	34.5	1	465	523	680	461	499	9.3	0.68

[a]DSC results; [b]TMA results

the Na^+ ions, the weakest point for water attack. An increase of chemical durability in compositional series B could be attributed to the increased number of Ti–O–P and Ti–O–Ti bonds with increasing TiO_2/P_2O_5 ratio.

Results from thermomechanical analysis are given in Table 1. It can be seen that incorporation of Ti^{4+} ions into the phosphate network results in a decrease of thermal expansion coefficient, α, of glasses while the glass transition temperature, T_g, and dilatation softening temperature, T_d, increase in both studied glass series. It was found that the values of α obtained from TMA measurements decrease slightly from 25.5 (x=2.5 mol% TiO_2) to 21.4 ppm $°C^{-1}$ (x=10) for the glass series A and steeply decrease from 22.0 (y=5) to 9.3 ppm $°C^{-1}$ (y=20 mol% TiO_2) for the glass series B (Fig. 2). The values of T_g in the metaphosphate glass series A increase with increasing TiO_2 content from 294°C for the glass with composition $47.5Na_2O–2.5TiO_2–50P_2O_5$ up to 331°C at the $40Na_2O–10TiO_2–50P_2O_5$ glass. In the series $45Na_2O–yTiO_2–(55–y)P_2O_5$ (B) the values of T_g shift from 307°C (y=5 mol% TiO_2) to 461°C (y=20) with the replacement of P_2O_5 by TiO_2. The dilatation softening temperature, T_d, was higher by 20–44°C than T_g values (Table 1). The observed increase in T_g and decrease in α show again the increasing bonding strength in the glass structure with increasing TiO_2 content.

DSC curves obtained for studied glass series are shown in Figs 1 and 2. The glass transition temperature, T_g (determined as the midpoint of the change in C_p in the glass transition region), the values of crystallization temperature, T_c, (the onset of the first crystallization peak) and the values of melting temperature, T_m, (onset of the first melting peak) were determined from DSC curves. The results are summarized in Table 1. It was found that compositional trends of T_g values in both glass series are similar to the trends in T_g determined from dilatation curves. From the DSC curves of the studied glasses we determined glass transition temperatures T_g which were higher by 1–4°C than the values obtained from dilatation curves.

From the DSC curves of the studied glasses it is also evident that all glasses crystallize on heating (Figs 1 and 2); some of them crystallize in several steps. The crystallization temperature, T_c (onset of the first crystallization peak) gradually increases in the temperature range of 316–464°C with TiO_2 content for the glass series of $(50–x)Na_2O–xTiO_2–50P_2O_5$ and in the temperature range of 432–523°C for the glasses with composition $45Na_2O–yTiO_2–(55–y)P_2O_5$. The crystalline phases obtained by the crystallization process start to melt within the range 592–610°C (for the A series) and from 600–680°C (B series; Table 1).

The obtained glasses were crystallized for 2 h in air at 20°C above the end of the last crystallization peak. The X-ray diffraction analysis showed that by heating the parent sodium metaphosphate glasses in compositional series A, crystalline $Na_3P_3O_9$ phase is formed. With increasing TiO_2 content, this compound is gradually replaced by crystalline $NaPO_3$, TiP_2O_7 and $NaTi_2(PO_4)_3$ phases (Fig. 3). In the glass series B

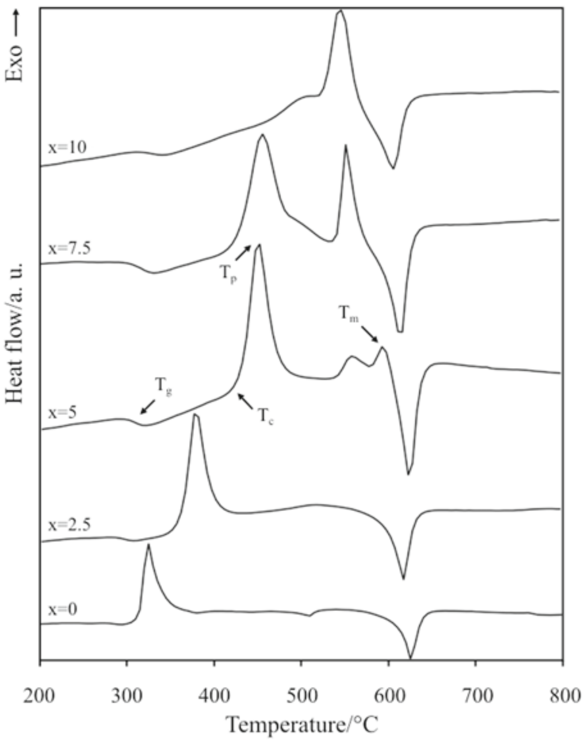

Fig. 1 DSC curves of the glass series $(50–x)Na_2O–xTiO_2–50P_2O_5$ (A)

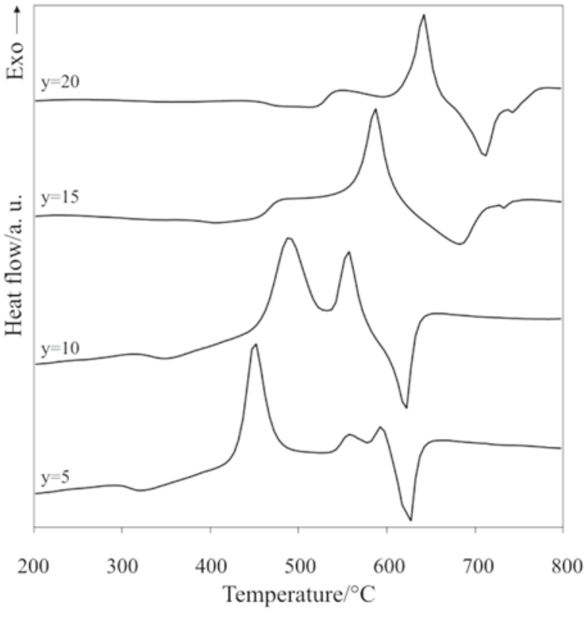

Fig. 2 DSC curves of the glass series $45Na_2O–yTiO_2–(55–y)P_2O_5$ (B)

(Fig. 4) we can see similar changes. Beside the crystalline phases described above, diffraction lines of $Na_5P_3O_{10}$ and $Na_4P_2O_7$ compounds were observed.

The mechanism of crystallization (surface or volume) was evaluated from the changes in the shape and position of the crystallization peak in DSC curves in dependence on the particle size (in our case 120, 300, 600 and 900 μm) of the studied glasses using the method suggested by Ray and Day [11]. This analysis was carried out only for the samples with the composition of $50Na_2O–50P_2O_5$, $45Na_2O–5TiO_2–50P_2O_5$, $42.5Na_2O–7.5TiO_2–50P_2O_5$ and $45Na_2O–10TiO_2–45P_2O_5$. From the DSC curves obtained at the heating rate of 10°C min^{-1} for different particle sizes, the peak crystallization temperature T_p, its maximum height, $(\delta T)_p$, and the width at the half-peak maximum, $(\Delta T)_p$, were determined. The ratio of the volume to the total effective surface area of all glass particles increases with an increasing particle size for a given amount of sample. Thus, the parameters $(\delta T)_p$ and $T_p^2/(\Delta T)_p$ should increase with increasing particle size when the internal crystallization predominates, while, for the dominant surface crystallization, the reverse effect should be observed [11]. The estimated parameter of $[(\delta T)_p]^R$ reduced to the sample with the lowest particle size of 130 μm (the values of $(\delta T)_p$ were divided by the values obtained with the smallest particle size; abbreviation R denotes reduced values), is plotted as a function of particle size in Fig. 5. As can be seen from the figure, the values of $[(\delta T)_p]^R$ continuously decrease with increasing particle size for all samples studied. These results suggest that the glasses nucleate predominantly by a surface crystallization mechanism. Similar conclusions can be drawn from the changes of $[(T_p^2/(\Delta T)_p)]^R$ reduced parameter as a function of particle size. From the changes in both $[(\delta T)_p]^R$ and $[(T_p^2/(\Delta T)_p)]^R$ parameters with particle size of analyzed glasses it is also evident that, with increasing TiO_2 content, the contribution of the surface crystallization mechanism increases. The highest contribution of internal crystallization mechanism was found in the parent $NaPO_3$ metaphosphate glass (Fig. 5). These conclusions are in good agreement with observed changes in T_g/T_m values as a function of TiO_2 content (Table 1). According to [12] when $T_g/T_m>0.6$, only surface crystallization is observed in laboratory time scales, while internal crystallization is easily observed in glasses where $T_g/T_m<0.6$.

The nucleation rate was studied by the method described in paper [13]. The method consists of heating the glass at different constant temperatures for a fixed time in DSC equipment before being crystallized at a fixed heating rate. A plot of the maximum DSC peak height, δT_p, as a function of the nucleation temperature, produced a nucleation-rate-like curve that determined the temperature range for nucleation and the temperature of the maximum nucleation rate [13]. As we can see in Fig. 6, for the glass composition $45Na_2O–5TiO_2–50P_2O_5$ (x, y=5), the peak height,

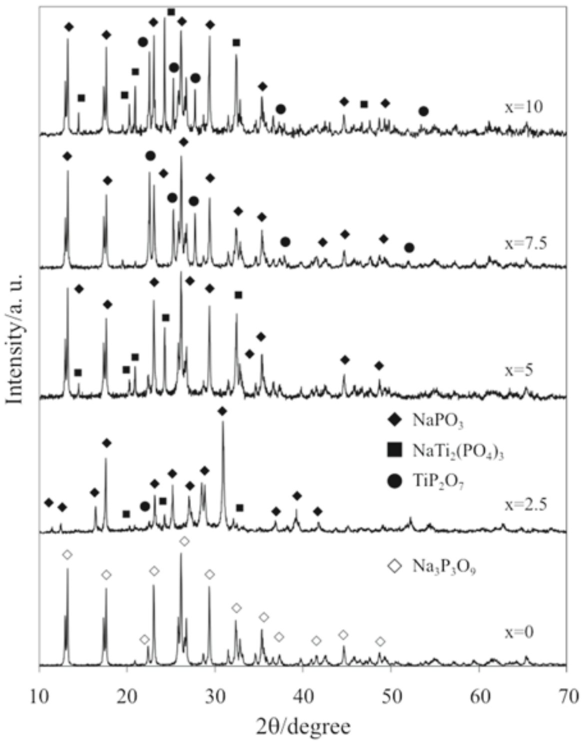

Fig. 3 X-ray diffraction patterns of the crystallized samples of the series $(50–x)Na_2O–xTiO_2–50P_2O_5$ (A)

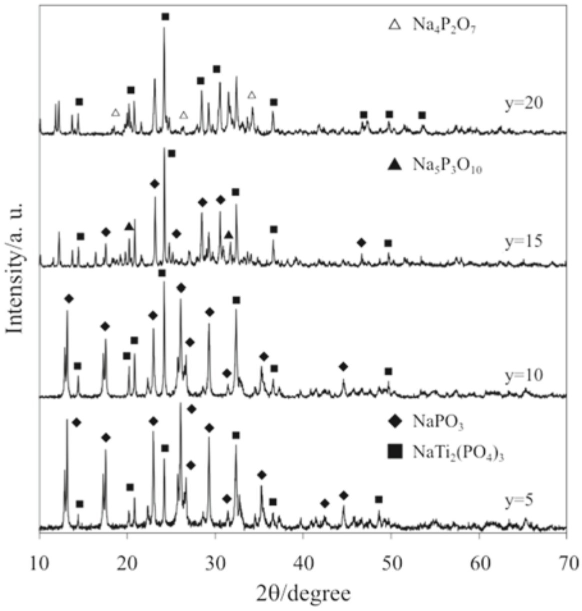

Fig. 4 X-ray diffraction patterns of the crystallized samples of the series $45Na_2O–yTiO_2–(55–y)P_2O_5$ (B)

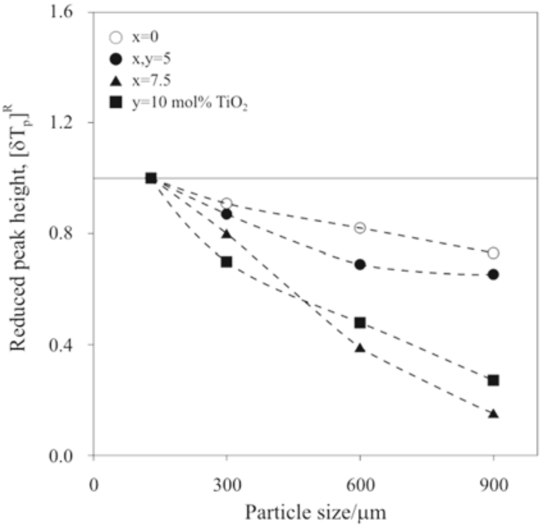

Fig. 5 Reduced values of peak height, $[(\delta T)_p]^R$, as a function of particle size for the (50–*x*)Na_2O–*x*TiO_2–50P_2O_5 (*x*=0, 5, 7.5 mol% TiO_2) and 45Na_2O–*y*TiO_2–(55–*y*)P_2O_5 (*y*=5, 10 mol% TiO_2) glasses.

δT_p, as a function of nucleating temperature, T_N, reveals a maximum at 350°C (for the heat treatment of 30 min). Nevertheless, for nucleating temperatures under 350°C, the nucleation rate is sufficient to produce many more nuclei than the number present in as-quenched glass. On the other hand for nucleating temperatures >350°C, the nucleation rate steeply decreases and for the samples nucleated at T_N close to T_c (432°C, Table 1) the crystallization peak practically disappears. The dependence of the peak temperature, T_p, on the nucleation time, t_N, (at T_N=350°C) for the same glass composition showed (Fig. 7), that T_p increases with increasing nucleating time from 15 min to a maximum at 30 min and then decreases sharply. This indicates that, after heating within the nucleation time region 15–45 min at 350°C, the majority of nuclei are formed. The study of nucleation rate of the other sodium titanophosphate glasses showed that the maximum of nucleation rate, $T_{N_{max}}$, is gradually shifted towards T_c and the nucleation time, t_N, (the time at which the peak temperature, T_p, as a function of t_N, reveals a maximum) increases with increasing TiO_2 content.

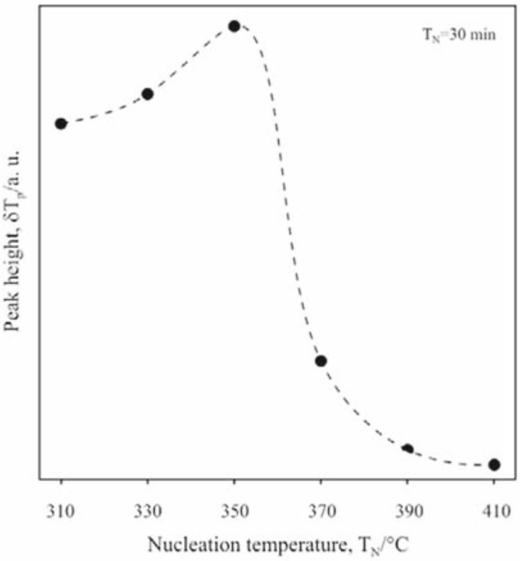

Fig. 6 The height, $(\delta T)_p$, of the DSC crystallization peak for the 45Na_2O–5TiO_2–50P_2O_5 glass as a function of nucleation temperature, T_N.

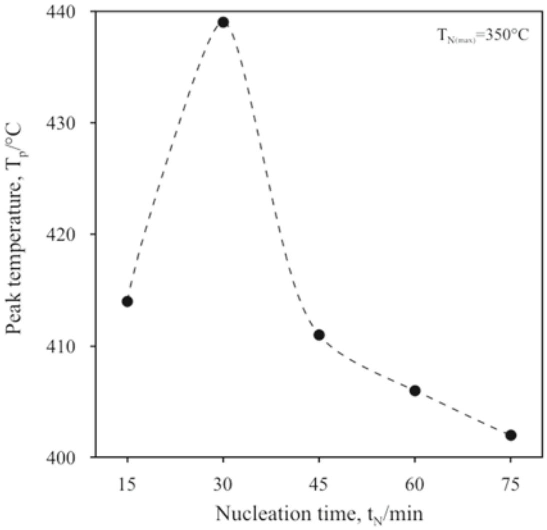

Fig. 7 Crystallization peak temperature, T_p, for the 45Na_2O–5TiO_2–50P_2O_5 glass as a function of nucleation time, t_N.

Conclusions

The study of $Na_2O–TiO_2–P_2O_5$ glasses revealed that replacement of Na_2O or P_2O_5 by TiO_2 leads to significant changes in the physico-chemical and thermal properties of these glasses. TMA and DSC measurements showed that the incorporation of TiO_2 into the structural network of the sodium phosphate glasses results in an increase of the glass transition temperature and the crystallization temperature. On the other hand, the thermal expansion coefficient of the glasses decreases with increasing titanium oxide content, particularly in the case of replacing P_2O_5 by TiO_2. Gradual strengthening of the phosphate network structure by titanate groups also results in a significant increase of chemical durability which is clearly an important factor in the commercial application of these glasses.

Acknowledgements

The authors are grateful for the financial support from the research project No. 0021627501 of the Ministry of Education of Czech Republic and to the Grant Agency of the Czech Republic (Grant No. 104/07/0315).

References

1 M. Navarro, M. Cinebra, J. Clément, S. Martínes, G. Avila and A. Planell, J. Am. Ceram. Soc., 86 (2003) 1345.
2 V. Rajendran, A. V. Gayathri Devi, M. Azzoz and F. H. El-Batal, J. Non-Cryst. Solids, 353 (2007) 77.
3 E. M. Vogel, S. G. Kosinski, D. M. Krol, J. L. Jackel, S. R. Fribert, M. K. Oliver and J. D. Powers, J. Non-Cryst. Solids, 107 (1989) 244.
4 G. D. L. K. Jayasinghe, P. W. S. K. Bandaranayake, M. A. K. L. Dissanayake and R. P. Gunawardane, Solid State Ionics, 78 (1995) 199.
5 L. Koudelka, P. Mošner, J. Pospíšíl, L. Montagne and G. Palavit, J. Solid State Chem., 178 (2005) 1837.
6 J. Pospíšil, P. Mošner and L. Koudelka, J. Therm. Anal. Cal., 84 (2006) 479.
7 K. Brow, D. R. Tallant, W. L. Warren, A. McIntyre and D. E. Day, Phys. Chem. Glasses, 38 (1997) 300.
8 S. Krimi, A. Eljazouli, L. Rabardil, M. Cousi, I. Mansouri and G. Le Flem, J. Solid State Chem., 102 (1993) 400.
9 L. Montagne, G. Palavit, A. Shaim, M. Et-Tabirou, P. Hartmann and Ch. Jäger, J. Non-Cryst. Solids, 293–295 (2001) 719.
10 A. Kishioka, M. Haba and M. Amagasa, Bull. Chem. Soc. Jpn., 47 (1974) 2493.
11 C. S. Ray and D. E. Day, Thermochim. Acta, 280–281 (1996) 163.
12 I. Avramov, E. D. Zanotto and M. O. Prado, J. Non-Cryst. Solids, 320 (2003) 9.
13 C. S. Ray, X. Fang and D. E. Day, J. Am. Ceram. Soc., 83 (2000) 865.

Received: October 20, 2008
Accepted: November 7, 2008
Online First: February 4, 2009

DOI: 10.1007/s10973-008-9584-z